

Cite this: *Chem. Sci.*, 2024, 15, 4179

All publication charges for this article have been paid for by the Royal Society of Chemistry

Rule breaker boron clusters: a new class of hypoelectronic osmaborane clusters $[(\text{Cp}^*\text{Os})_2\text{B}_n\text{H}_n]$ ($n = 6-10$)[†]

Ketaki Kar, Sourav Kar and Sundargopal Ghosh *

Since the pioneering electron counting rule for borane clusters was proposed by Wade, the structures and bonding of boron clusters and their derivatives have been elegantly rationalised. However, this rule and its modified versions faced problems explaining the electronic structures of less spherical deltahedra, unlike the core geometries of borate dianions $[\text{B}_n\text{H}_n]^{2-}$ ($n = 6-12$). Herein, we report the isolation of a series of osmaborane clusters $[(\text{Cp}^*\text{Os})_2\text{B}_n\text{H}_n]$, 1–5, ($n = 6-10$) by the thermolysis of an *in situ* generated intermediate, obtained from the rapid condensation of $[\text{Cp}^*\text{OsBr}_2]_2$ and $[\text{LiBH}_4 \cdot \text{THF}]$, with $[\text{BH}_3 \cdot \text{THF}]$ or $[\text{BH}_3 \cdot \text{SMe}_2]$. Interestingly, all these clusters show unusual less spherical deltahedral shapes that can be generated from canonical $[\text{B}_n\text{H}_n]^{2-}$ ($n = 8-12$) shapes by doing diamond-square-diamond (DSD) rearrangements. The DSD rearrangements led to the generation of higher degree vertices, which are occupied by Os atoms and also generated Os–Os bonds in these clusters. Theoretical calculations revealed that these $\text{Cp}^*\text{Os} \cdots \text{OsCp}^*$ interactions in clusters 1–5 played a crucial role in their structural shape and electron count. These less spherical deltahedral clusters are rare, and most significantly, clusters 1–5 with $(n-1)$ skeleton electron pairs (SEPs) do not follow Wade–Mingos electron counting rules and can be classified as hypoelectronic *closo* clusters.

Received 2nd December 2023
Accepted 6th February 2024

DOI: 10.1039/d3sc06464f

rsc.li/chemical-science

Introduction

Wade's electron-counting approach¹ has been pivotal in the growth of main group and transition metal cluster chemistry since its appearance in 1971.^{2,3} Subsequently, Williams, Mingos, and Jemmis modified this approach and introduced electron-counting rules for single and fused polyhedral clusters.⁴ The effectiveness of these cluster electron-counting rules, combined with the isolobal analogy,⁵ in explaining the majority of cluster framework acclaimed considerable credence. In particular, most of the cluster shapes are classified and rationalised as *closo* [$(n+1)$ SEP], *nido* [$(n+2)$ SEP], *arachno* [$(n+3)$ SEP], and *hypho* [$(n+4)$ SEP] based on the structural and electronic properties of these compounds (SEP = skeleton electron pair). In this regard, metallaboranes constitute a class of compounds intermediate between borane cages on one hand and transition metal clusters on the other. Thus, they provide a test bed for the evaluation of electronic compatibility or incompatibility of metal and borane fragments. However, most of the late transition metal metallaborane clusters exhibit the

usual *closo*, *nido*, and *arachno*-deltahedral shapes and obey the electron counting rules.^{2b,c,3a,6}

In contrast, Hawthorne, Kennedy, Fehlner, and our group have isolated some metallaborane clusters that have unusual structures and different electron counts.^{7,8} In particular, these unusual clusters have one or more degree 6 vertices, whereas the corresponding regular borane $[\text{B}_n\text{H}_n]^{2-}$ ($n = 6-12$) deltahedra have only degree 4 and 5 vertices (except $[\text{B}_{11}\text{H}_{11}]^{2-}$ that has a degree 6 vertex).⁹ Usually, these higher degree 6 vertices in metallaborane clusters are occupied by transition metals owing to their diffuse orbitals.¹⁰ Interestingly, these unusual clusters have less SEP count and do not follow the electron counting rule. Usually, these closed deltahedra with unusual geometries have one less SEP count, which are classified as *isocloso* or *hypercloso* (n SEP).^{7e,11} In 1975, Hawthorne and co-workers isolated the first *isocloso*-cluster, $[(\text{FeCp})_2\text{B}_6\text{C}_2\text{H}_8]$.¹² However, it was not recognised as an *isocloso*-cluster at that time. Later on, Kennedy and co-workers recognised the structural and electronic uniqueness of such *isocloso*-clusters.^{7c,d} Thereafter, various research groups, for example, Hawthorne, Kennedy, Fehlner, and us isolated many *isocloso*, and *isonido*-metallaborane and metallacarborane clusters (Chart 1).^{7,8} These *isocloso* polyhedral structures can be derived from the corresponding *closo* deltahedron by DSD rearrangements (Chart 1).^{11a,13} For example, Kennedy and co-workers isolated and structurally characterized an *isocloso*-10-vertex metallaborane cluster $[(\text{PPh}_3)\text{RuHCl}]\text{B}_9\text{H}_7(\text{PPh}_3)_2$ (**1**), which has 10

Department of Chemistry, Indian Institute of Technology Madras, Chennai 600036, India. E-mail: sghosh@iitm.ac.in

[†] Electronic supplementary information (ESI) available. CCDC numbers 2291109 (for 1), 2293942 (for 2), 2300469 (for 3), 2291111 (for 4), and 2291112 (for 5). For ESI and crystallographic data in CIF or other electronic format see DOI: <https://doi.org/10.1039/d3sc06464f>

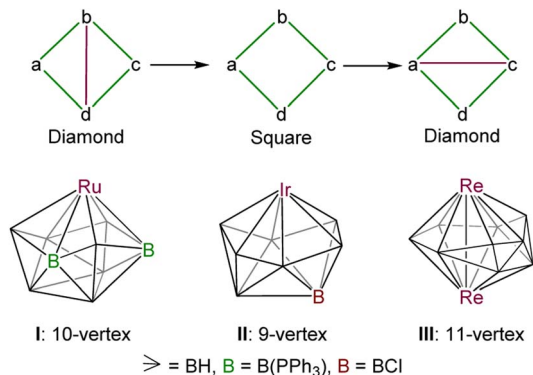


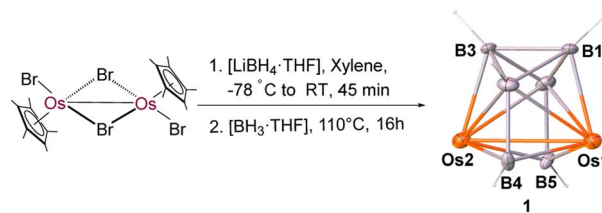
Chart 1 (Above) Diamond–Square–Diamond (DSD) rearrangement. (Below) examples of various hypoelectronic metallaborane clusters with unusual structures. Ru = [RuHCl(PPh₃)], Ir = [IrH(PMe₃)₂], Re = [ReCp*].

SEP.¹⁴ The structural shape of the *isocloso*-cluster **I** can be generated from the corresponding *closo*-geometry (bicapped square antiprism) by doing a DSD rearrangement, whereas a 9-vertex-*isocloso*-cluster, [(PMe₃)₂IrH]B₈H₇Cl (**II**; 9 SEP), can be generated from the corresponding *closo*-geometry (tricapped trigonal prism) by doing two successive DSD rearrangements.¹⁵ On the other hand, Fehlner and co-workers isolated a series of hypoelectronic dirhenaborane clusters [(Cp*Re)₂B_nH_n] (*n* = 7–10) having unusual cores and (*n* – 2) SEP that can be generated using two or more than two DSD rearrangements and Re–Re bond formations.^{8a}

In this regard, although our search for the isolation of hypoelectronic clusters led to the synthesis of various metallaborane clusters, most of them have regular deltahedral cores.^{3a} Recently, we have synthesised and structurally characterised hypoelectronic isomeric diiridaboranes [(Cp*Ir)₂B₆H₆] having dodecahedron and bicapped trigonal prism cores.¹⁶ As heavier transition metals of groups 7 and 9 (Re and Ir) led to the isolation of hypoelectronic metallaborane clusters with unusual geometries, we have investigated the metallaborane chemistry of their neighbouring heavier metal osmium. Indeed, we are able to isolate a series of hypoelectronic osmaboranes utilizing [Cp*OsBr₂]₂ and various borane reagents, such as [LiBH₄·THF], [BH₃·THF], and [BH₃·SMe₂].

Results and discussion

Reaction of [Cp*OsBr₂]₂ with four equivalents of [LiBH₄·THF] at –78 °C followed by thermolysis at 110 °C in the presence of an excess of [BH₃·THF] for 16 h led to the formation of a colorless solid **1** along with a few air and moisture sensitive unstable products (Scheme 1). The room-temperature ¹¹B{¹H} NMR spectrum of **1** showed three chemical shifts between a wide range of δ = –16.3 and +97.4 ppm with equal intensities. The ¹H NMR spectrum of **1** suggests the existence of a single Cp* environment appearing at δ = 2.03 ppm. In addition, the ¹H NMR spectrum also shows the existence of three chemical shifts at δ = 9.92, 8.97 and –2.31 ppm for terminal B–H hydrogens, which were further confirmed by ¹H{¹¹B} NMR. The mass



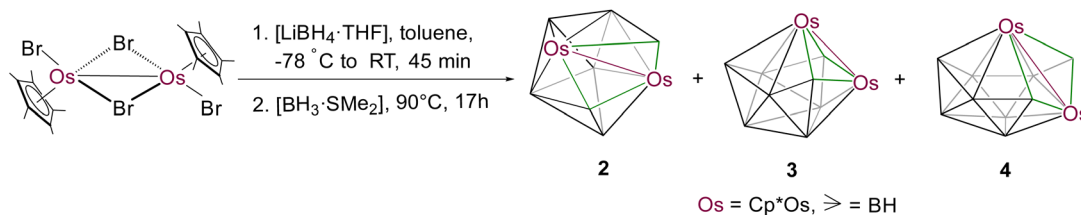
Scheme 1 Synthesis of hypoelectronic closed osmaborane cluster **1**. Note that Cp* ligands attached to Os atoms of the molecular structure of **1** are omitted for clarity. Selected bond lengths (Å) and angles (°) of **1**: Os1–Os2 2.7688(3), Os1–B4 2.055(8), Os1–B5 2.060(7), Os2–B4 2.062(7), Os2–B5 2.084(8), B4–Os1–Os2 47.9(2), Os1–B4–Os2 84.5(3).

spectrum showed a molecular-ion peak at *m/z* 745.2463 [(M + Na)⁺]. All these spectroscopic data were not adequate enough to envisage the molecular structure of **1**. Therefore, we have carried out the single-crystal X-ray structure analysis on a suitable crystal of **1**.

Single crystal X-ray analyses revealed **1** as a closed 8-vertex-osmaborane cluster [(Cp*Os)₂B₆H₆] (Scheme 1). Interestingly, the {Os₂B₆} core geometry of **1** is different from that of the corresponding dodecahedron [B₈H₈]^{2–}. The presence of an Os–Os bond and the absence of a B–B bond in cluster **1** make the difference with the canonical dodecahedron [B₈H₈]^{2–}. The Os–Os bond distance of 2.7688(3) Å in **1** is slightly longer than that of [(Cp*Os)₃(μ-H)₆][BPh₄] (Os–Os: 2.7212(2), 2.7096(2), and 2.7168(2) Å) and [(Cp*Os)₃(μ-H)₃(μ₃-H)₂] (Os–Os: 2.7181(4), 2.7190(3), and 2.7286(3) Å).¹⁷ On the other hand, all the Os–B and B–B bond distances of cluster **1** are comparable with that of reported osmaboranes.¹⁸ Interestingly, the presence of Os–Os bond reduces the number of symmetry elements of the core geometry of **1** in comparison with their canonical symmetric deltahedra [B_nH_n]^{2–}. For example, cluster **1** has one C₂ axis passing through the midpoints of B1–B6 and Os1–Os2 bonds and two σ_v planes in which one bisects the B1–B6 and Os1–Os2 bonds and the other passes through these bonds, whereas the canonical *closo*-dodecahedron [B₈H₈]^{2–} has higher D_{2d} symmetry.

In metallaborane cluster chemistry, the sources of boron play a pivotal role in the isolation of different types of metallaboranes with unusual structural motifs. Thus, we have revised the synthetic methodology with different borane sources and used [BH₃·SMe₂] instead of [BH₃·THF]. As a result, the reaction of [Cp*OsBr₂]₂ with four equivalents of [LiBH₄·THF] at –78 °C followed by thermolysis at 90 °C in the presence of [BH₃·SMe₂] led to the isolation of a series of hypoelectronic closed osmaboranes, 9-vertex-[(Cp*Os)₂B₇H₇] (**2**), 10-vertex-[(Cp*Os)₂B₈H₈] (**3**), and 11-vertex-[(Cp*Os)₂B₉H₉] (**4**) (Scheme 2). Further increase of temperature to 110 °C, albeit of similar time, allowed us to isolate 12-vertex-[(Cp*Os)₂B₁₀H₁₀] (**5**) in very low yield. All these new compounds were characterised by ¹H, ¹H{¹¹B}, ¹¹B{¹H}, and ¹³C{¹H} NMR, IR spectroscopy, mass spectrometry, and single crystal X-ray analysis. Note that along with the formation of clusters 2–5, the reaction also yielded some air and moisture-sensitive ionic products, which are quite unstable for isolation.





Scheme 2 Synthesis of hypoelectronic closed osmaborane clusters 2–4.

Clusters 2–5 were isolated as dark green, orange, violet and green solids, respectively. The $^{11}\text{B}\{^1\text{H}\}$ NMR of **2** showed five chemical shifts, which appeared in a wide range of $\delta = 6.2$ to 107.7 ppm with unequal intensities, whereas **3** and **4** showed eight and nine $^{11}\text{B}\{^1\text{H}\}$ NMR chemical shifts with equal intensities in the ranges of $\delta = -13.0$ to 89.3 ppm and $\delta = 2.4$ to 95.9 ppm, respectively. Cluster **5** showed four $^{11}\text{B}\{^1\text{H}\}$ chemical shifts within the range of $\delta = -8.7$ to 43.9 ppm with unequal intensities. The ^1H NMR spectra of **2** and **5** suggest the existence of a single Cp^* environment appearing at $\delta = 1.96$ and 1.93 ppm, respectively, whereas the ^1H NMR spectra of **3** and **4** showed the presence of two different Cp^* environments at $\delta = 1.97$ and 1.79 ppm (for **3**) and at $\delta = 1.84$ and 1.82 ppm (for **4**) with equal intensities. Besides, the ^1H NMR spectra of **1**–**5** revealed the existence of broad chemical shifts in the deshield zones due to the presence of terminal B–H hydrogens. Furthermore, the mass spectra of **2**–**5** showed molecular-ion peaks at m/z 735.2891 $[(\text{M} + \text{H})^+]$, m/z 784.3152 $[(\text{M} + \text{K})^+]$, m/z 789.3471 $[(\text{M} + \text{CH}_3\text{OH})^+]$, and m/z 770.3433 $[(\text{M} + \text{H})^+]$, respectively. The mass spectrometric data of **1**–**5** indicate that a $\{\text{BH}\}$ unit is added at each step when one moves from **1**–**5** sequentially. Although higher molecular-ion peaks and NMR spectra of **2**–**5** specify the formation of osmaborane clusters, these spectroscopic data were not sufficient to envisage the identity of these clusters. A clear explanation eluded us until solid-state single-crystal X-ray structure analyses of **2**–**5** were carried out.

The single crystal X-ray diffraction analyses revealed **2**–**5** as closed 9–12-vertex osmaborane clusters, *i.e.*, $[(\text{Cp}^*\text{Os})_2\text{B}_7\text{H}_7]$, $[(\text{Cp}^*\text{Os})_2\text{B}_8\text{H}_8]$, $[(\text{Cp}^*\text{Os})_2\text{B}_9\text{H}_9]$, and $[(\text{Cp}^*\text{Os})_2\text{B}_{10}\text{H}_{10}]$,

respectively (Fig. 1 and 2). Interestingly, the core geometries of these clusters are unusual and different from those of the corresponding deltahedra $[\text{B}_n\text{H}_n]^{2-}$ ($n = 9$ – 12). For example, all these clusters have strong Os–Os bonds with bond distances of 2.8051(5) Å (**2**), 2.9046(11) Å (**3**), 2.8505(7) Å (**4**), and 2.832(2) Å (**5**). Interestingly, all the Os–B and B–B bond distances of clusters **2**–**5** are in accord with that of reported osmaboranes.¹⁸ Like cluster **1**, the presence of Os–Os bonds in clusters **2**–**5** reduces the number of symmetry elements of the core geometries of **2**–**5** in comparison with their canonical symmetric deltahedra $[\text{B}_n\text{H}_n]^{2-}$. For example, 10-vertex cluster **3** lost most of its symmetry elements compared to its canonical bicapped square antiprism $[\text{B}_{10}\text{H}_{10}]^{2-}$ isomer (D_{4d} symmetry). It has only one σ -plane that passes along the Os1–Os2 and B1–B2 bonds and bisects the B8–B6 bond. Also, the isomer of one of the most symmetric icosahedra, 12-vertex cluster **5**, has one C_2 axis passing through the midpoints of B4–B7 and Os1–Os2 bonds and two σ_v planes in which one bisects the B4–B7 and passes through Os1–Os2 bonds and another bisects B8–B10, Os1–Os2 and B2–B6 bonds. Clusters **2** and **4** do not have any symmetry, whereas the corresponding *closo*-tricapped trigonal prism $[\text{B}_9\text{H}_9]^{2-}$ and *closo*-octadecahedron $[\text{B}_{11}\text{H}_{11}]^{2-}$ have D_{3h} and C_{2v} symmetry, respectively.

The observed core geometries of clusters **1**–**5** are clearly different from those of the parent deltahedra of $[\text{B}_n\text{H}_n]^{2-}$ ($n = 8$ – 12), however they can be related to the canonical shapes by DSD rearrangements (Fig. 3). In all cases, the total vertex connectivities (tvc) and total triangular faces of clusters **1**–**5** are the same as those of the canonical deltahedra of $[\text{B}_n\text{H}_n]^{2-}$ (Table 1). Clusters **1**–**5** exhibit a greater number of higher and lower-

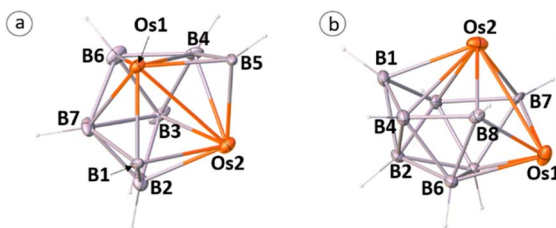


Fig. 1 Molecular structures and labelling diagrams of clusters **2** (a), and **3** (b). Note that Cp^* ligands attached to Os atoms are omitted for clarity. Selected bond lengths (Å) and angles ($^\circ$) of **2**: Os1–Os2 2.8051(5), B1–Os1 2.081(12), B5–Os1 2.030(11), B1–Os2 2.180(11), B4–B5 1.78(2), B3–B4 1.76(2), Os1–B5–Os2 87.1(5), B1–Os1–Os2 50.4(3); **3**: Os1–Os2 2.9046(11), Os2–B8 2.14(3), Os1–B8 2.13(3), Os1–B7 2.22(4), Os2–B7 2.16(3), B2–B6 1.78(5), B4–B8 1.73(6), Os1–B8–Os2 85.7(11).

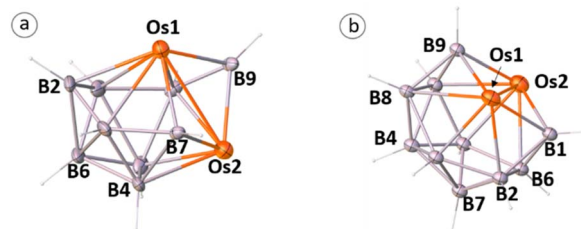


Fig. 2 Molecular structures and labelling diagrams of clusters **4** (a) and **5** (b). Note that Cp^* ligands attached to Os atoms are omitted for clarity. Selected bond lengths (Å) and angles ($^\circ$) of **4**: Os1–Os2 2.8505(7), Os1–B7 2.159(17), Os1–B9 2.175(17), Os2–B9 2.051(18), B2–B6 1.82(3), B7–Os1–B9 91.4(7), Os2–B7–Os1 83.1(6); **5**: Os1–Os2 2.832(2), B1–Os1 2.14(4), B9–Os2 2.16(4), B2–B6 1.79(6), B4–B8 1.64(5), Os2–B9–Os1 81.3(15), B9–Os2–Os1 49.9(11).

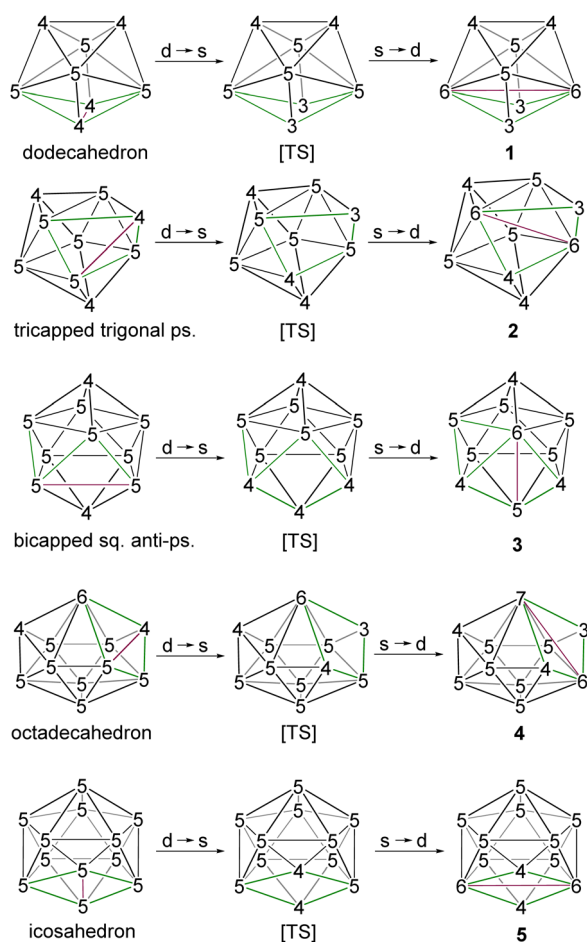


Fig. 3 Diamond-Square-Diamond (DSD) rearrangement of parent *closo*-clusters to form corresponding hypoelectronic clusters 1–5. ps. = prism, sq. = square.

Table 1 Structural comparison of clusters 1–5 with regular borate dianion $[B_nH_n]^{2-}$ ($n = 8–12$) clusters^a

Clusters	Deg-3	Deg-4	Deg-5	Deg-6	Deg-7	tvc	Δ
1	2	2	2	2	0	36	12
$[B_8H_8]^{2-}$	0	4	4	0	0	36	12
2	1	3	3	2	0	42	14
$[B_9H_9]^{2-}$	0	3	6	0	0	42	14
3	0	3	6	1	0	48	16
$[B_{10}H_{10}]^{2-}$	0	2	8	0	0	48	16
4	1	2	6	1	1	54	18
$[B_{11}H_{11}]^{2-}$	0	2	8	1	0	54	18
5	0	2	8	2	0	60	20
$[B_{12}H_{12}]^{2-}$	0	0	12	0	0	60	20


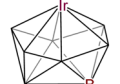
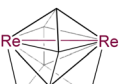
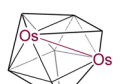


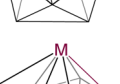




^a Deg = degree, Δ = number of triangle faces.

degree vertices than the canonical shapes (Table 1). The higher degree vertices of these cores in 1–5 are occupied by osmium atoms, which may be attributed to the diffused orbitals of heavier metals like osmium. For example, two degree-6 vertices in cluster 1 are occupied by osmium atoms, which generated an unusual 8-vertex closed polyhedral shape. Similarly, cluster 2

has two degree-6 vertices that are occupied by osmium atoms. Interestingly, apart from a higher degree-6 vertex, 11-vertex cluster 4 has a more connected degree-7 vertex, and both vertices are occupied by the heavier metal osmium. In the case of cluster 3, the higher degree vertices (one degree-6 and one degree-5) are occupied by osmium atoms, similar to that of iridaborane $[(Cp^*Ir)_2B_8H_8]$. Although 9–11-vertex clusters that underwent DSD rearrangement(s) are known, all of them have shapes like clusters I–III (Chart 1). Thus, to the best of our knowledge, the core geometries of clusters 1, 2 and 4 are the first of its types. On the other hand, 12-vertex cluster 5 has two degree-6 vertices that are occupied by osmium atoms. A similar cluster shape to that of cluster 5 was observed for two group 9 heavier metals, metallaboranes $[(Cp^*M)_2B_{10}H_{12}]$ ($M = Rh$ or Ir).^{6c,19} However, the electron count of these two rhoda- and iridaborane clusters (13 SEP) strongly differ from that of cluster 5 having 11 SEP (*vide infra*). Another significant prospect of these unusual clusters 1–5 is the flattened faces along the Os–Os vectors. The dihedral angles along B4–Os1–Os2–B5 in 1 is 145.33° , along B1–Os1–Os2–B5 in 2 is 152.17° , along Os1–B7–B8–Os2 in 3 is 152.11° , along B7–Os1–Os2–B9 in 4 is 156.61° , and along B1–Os1–Os2–B9 in 5 is 176.39° . This flattening brings the Os atoms closer together in clusters 1–5 to form Os–Os bonds and formed oblate shape clusters. Similar types of flattening along the faces where DSD rearrangements took place are observed in *oblato*-clusters.^{8a,e,20} For example, the dihedral angle along B–Fe–Fe–C in *isocloso*- $[(Cp)Fe]_2B_6C_2H_8$ ¹² is 149.87° , along B–Ir–Ir–B in $[(Cp^*Ir)_2B_{10}H_{12}]$ ^{6c} it is 173.30° and along Ti–B–B–Ti in *oblato-hypho*- $[(Cp^*Ti)_2B_{14}H_{18}]$ ^{8e} it is 175.7° . Thus, clusters 1–5 can also be classified as *oblato*-clusters. Another uniqueness of these osmaborane clusters is that despite metals (Os and Ru) of the same triad, their structures differ from diruthenaboranes. While these osmaboranes have closed geometries, most of the diruthenaboranes have open geometries with *nido/arachno* shapes.

The single-crystal X-ray structures are also consistent with the $^{11}B\{^1H\}$, $^1H\{^{11}B\}$, and $^{13}C\{^1H\}$ NMR spectra of clusters 1–5. For example, the presence of one C_2 axis and two σ_v planes in cluster 1 is also evident from the single 1H chemical shift for two Cp^* ligands attached to Os atoms. Furthermore, three $^{11}B\{^1H\}$ chemical shifts at $\delta = 97.4$, 61.3 and -16.3 ppm with equal intensities represent three sets of boron atoms in 1 [(B4, B5); (B1, B6); and (B2, B3), respectively]. Similarly, the presence of one C_2 axis and two σ_v planes in cluster 5 is reflected in its 1H , $^{13}C\{^1H\}$ and $^{11}B\{^1H\}$ NMR spectra. Due to the presence of these symmetry elements, four sets of boron atoms in 5 [(B1, B9); (B3, B5); (B4, B7); and (B2, B6, B8, B10)] showed four different $^{11}B\{^1H\}$ NMR environments that appeared at $\delta = 43.9$, 16.1, 4.6 and -8.7 ppm with an intensity ratio of 2 : 2 : 2 : 4. On the other hand, clusters 2 and 4 have the C_1 point group. Thus, these clusters have no symmetry elements except the trivial C_1 axis, which is also reflected in their 1H and/or $^{13}C\{^1H\}$ NMR chemical shifts with two Cp^* environments. The $^{11}B\{^1H\}$ NMR of cluster 4 showed nine chemical shifts with equal intensities for nine boron environments. However, we observed five ^{11}B chemical shifts for cluster 2 ($\delta = 107.7$, 77.7, 61.2, 56.0, and 6.2 ppm) with intensity ratios of 1 : 1 : 2 : 2 : 1 for seven boron environments in

Table 2 Structural parameters, electron count and spectroscopic details of different types of non-spherical clusters

Clusters	SEP	Degree		d_{M-M} (Å)	$d_{avg,M-B}$ (Å)	$d_{avg,B-B}$ (Å)	^{11}B NMR (ppm)	Ref.
		Highest	Lowest					
8-Vertex 	7	6	3	2.7688(3)	2.164	1.735	−16.3 to 97.4	This work
	9	6	4	—	2.227	1.757	a	15
9-Vertex 	7	7	4	2.7875(6)	2.163	1.756	3.6 to 101.7	8a, 21
	8	6	3	2.8051(5)	2.143	1.757	6.2 to 107.7	This work
	10	6	4	2.571(1)	2.102	1.815	−142.9 to 8.5	12
10-Vertex 	8	7	4	2.8345(8)	2.184	1.801	21.9 to 97.9	8a
	9 (Os) 10 (Ir)	6	4	2.9046(11) (Os) 2.802 (Ir)	2.232 (Os) 2.170 (Ir)	1.800 (Os) 1.764 (Ir)	−13.0 to 89.3 (Os) −10.6 to 81.9 (Ir)	19, this work
	9	8	4	2.8604(5)	2.209	1.751	−28.7 to 94.1	8a
11-Vertex 	10	7	4	2.8505(7)	2.193	1.750	2.4 to 95.9	This work
	10	8	4	2.8192(1)	2.237	1.721	−22.9 to 60.0	8a
12-Vertex 	11	6	4	2.832(2)	2.228	1.730	−8.7 to 43.9	This work

cluster 2. This may be due to the close proximity of chemical shifts of the two sets of boron atoms. On the other hand, although a symmetry plane can be drawn only by considering the $\{Os_2B_8\}$ core of cluster 3, the symmetry plane is lost due to the tilted ^{11}B NMR: range of ^{11}B chemical shifts, a = data not available, Os = $\{OsCp^*\}$, Ir = $\{IrH(PMe_3)_2\}$, B = $\{BCl\}$, Re = $\{ReCp^*\}$, Fe = $\{FeCp\}$, C = $\{CH\}$, Ir = $\{IrCp^*\}$ orientation of Cp^* ligands attached to Os atoms. This unsymmetric nature of cluster 3 is also reflected in their 1H NMR (two Cp^*

environments) and $^{11}B\{^1H\}$ NMR (eight $^{11}B\{^1H\}$ chemical shifts). Furthermore, the $^1H\{^{11}B\}$ NMR spectra of 1–5 revealed the presence of terminal B–H hydrogens in clusters 1–5, which were further confirmed by IR spectra.

Electron count and bonding of hypoelectronic osmaboranes 1–5

Based on the unique structural features of clusters 1–5, their electron count and bonding analysis become of interest. Usually, Wade–Mingos electron-counting rules are very useful



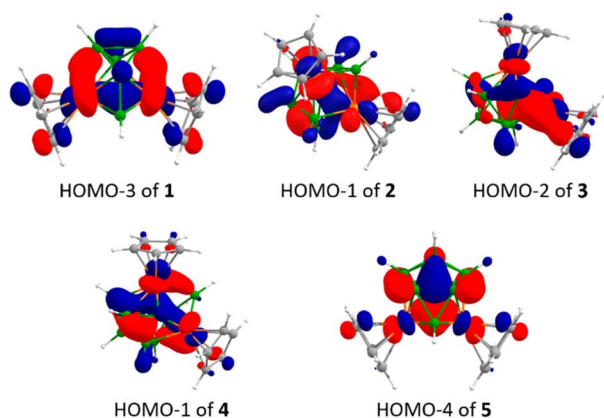


Fig. 4 Selected molecular orbitals of osmaborane clusters 1–5 depicting Os–Os, Os–B and B–B bonding interactions throughout the clusters. (Isocontour values: ± 0.043 [e bohr $^{-3}$] $^{1/2}$).

in predicting and systematising metallaborane clusters.^{1,3b,c} However, clusters that are generated by DSD rearrangement(s) from the canonical spherical $[B_nH_n]^{2-}$ ($n = 6-12$) also show defects in electron count relative to the Wade–Mingos rules (Table 2).^{11a} In most of the cases of DSD rearrangements, the closed clusters have n SEP instead of $(n + 1)$ SEP and are classified as *isocloso*/*hypercloso* clusters. However, clusters 1–5 have $(n - 1)$ SEP, which is 2 SEP less than that of canonical *closo* geometry (Table 2). For example, 8-vertex 1 has 7 SEP, 9-vertex 2 has 8 SEP, 10-vertex 3 has 9 SEP, 11-vertex 4 has 10 SEP, and 12-vertex 5 has 11 SEP. Here, each $\{Cp^*Os\}$ unit contributes 0.5 SEP, and each $\{BH\}$ unit contributes 1 SEP towards the cluster's skeleton electron pair count of 1–5. Thus, clusters 1–5 can be classified as hypoelectronic *closo*-clusters with $(n - 1)$ SEPs.

To investigate the bonding features and electronic structures of these unusual hypoelectronic clusters 1–5, we have carried out the theoretical analyses at the bp86/def2-SVP level of theory. The single crystal X-ray structural parameters of clusters 1–5 nicely corroborate with their optimised structural parameters (Table S1†). The MO analyses show larger HOMO–LUMO energy gaps for clusters 1, 2, and 4 of 3.33 eV, 2.03 eV, and 2.32 eV, respectively, which indirectly suggest kinetic and thermodynamic stability, whereas the HOMO–LUMO energy gaps for 10-vertex cluster 3 of 0.52 eV and for 12-vertex cluster 5 of 0.85 eV are shorter compared to that of clusters 1, 2, and 4. The MO analysis of 1–5 showed strong Os–Os interactions in all clusters. For example, HOMO-3 of 1 showed that the d_z^2 orbitals of two osmium metals participate in bonding interaction to form an Os–Os bond in cluster 1 (Fig. 4). Similarly, HOMO-1, HOMO-2, HOMO-1, and HOMO-4 of clusters 2–5, respectively, show the Os–Os bonding interactions through the overlap of d-orbitals of osmium metals (Fig. 4). Furthermore, the natural bond order (NBO) analysis revealed the Wiberg bond index (WBI) for Os...Os interactions (1: 0.367; 2: 0.371; 3: 0.756; 4: 0.351; 5: 0.836), which supported the MO findings of Os–Os bonding interactions. These Os–Os bonds in clusters 1–5 play a pivotal role in the rearrangement in shape as well as the number of cluster bonding orbitals and electron counting. In addition, the MO analysis shows the existence of extended delocalised bonding

interactions between the constituents of the clusters through Os–B and B–B bonds.

The experimental as well as theoretical studies of these new $[(OsCp^*)_2B_nH_n]$ clusters revealed that the number of bonded edges and total connectivity remained the same after DSD rearrangement with the generation of higher connectivity vertices. As a necessary consequence, this new class of clusters became less spherical compared to its canonical regular polyhedral $[B_nH_n]^{2-}$ clusters. This rearrangement process also permits the formation of an Os–Os bond, however, with the cost of a B–B bond. The $Cp^*M \cdots MCp^*$ interaction generated a set of FMOs that interact with available borane fragment orbitals to form strong bonding and antibonding MOs.^{8a} Thus, the M–B interaction increases and B–B interaction decreases in these types of noncanonical structures, but the total number of vertex-connectivities remained the same. Also, formation of a metal–metal bond demands additional bonding orbitals in these clusters, which is compensated at the expense of a non-spherical shape. Thus, the diffused orbitals of Os were beneficial in two ways for the stabilization of the non-spherical cores of 1–5 by providing higher connectivities and forming Os–Os bonds. As a result, a never-before seen low electron count is observed for this new class of boron clusters.

In order to investigate the optical properties of 1–5, we carried out UV-vis absorption studies. As shown in Fig. S34,† all the clusters display absorption peaks in the range of $\lambda = 230-260$ nm. This region is well known for the $\pi-\pi^*$ electronic transition of the pentamethylcyclopentadienyl ligand. In addition, cluster 1 showed one more low intense absorption peak at $\lambda = 342$ nm. The coloured clusters 2–5 showed more than one absorption peaks in the region of $\lambda = 315-524$ nm. The time-dependent DFT calculation (Fig. S40–S44 and Tables S3–S7†) suggested that these absorption peaks can be assigned to the electronic transitions that correspond to electron density flow from Os metals or Os–Os bond to the B–B and Os–B bonds.

Conclusions

In summary, we have synthesised and structurally characterised a series of hypoelectronic clusters 1–5. Interestingly, all these clusters have unique structural shapes that are different from canonical symmetric isomers $[B_nH_n]^{2-}$ ($n = 8-12$). The core geometries of these clusters can be associated with canonical symmetrical deltahedral cores by doing DSD rearrangements. This, in turn, generated Os–Os bonds and as a result, interfered with their electron counts. Clusters 1–5 with $(n - 1)$ SEP become two SEP less than the usual *closo*-clusters. As a result, they do not follow the Wade–Mingos electron counting rules and are classified as hypoelectronic *closo*-clusters. In view of the many recent efforts to obtain polyhedral clusters with unique structural motifs, this is a significant development in the chemistry of boron and there is no doubt that this will accelerate discoveries of unusual rule-breaking structures.

Data availability

The data that support the findings of this study are available in the ESI† of this article.



Author contributions

K. K. executed the experimental synthesis, characterisation and analysed the data. S. K. also analysed the data and carried out theoretical calculations. S. K. prepared the first draft of the manuscript. All authors contributed to the preparation of the manuscript. S. G. supervised the project.

Conflicts of interest

There are no conflicts to declare.

Acknowledgements

Generous support of Exploratory Research Funding, IIT Madras, Grant No. RF/2223/0528/CY/RFER/008224, and the Centre of Excellence on Molecular Materials and Functions under the Institution of Eminence scheme of IIT Madras is gratefully acknowledged. K. K. thanks DST-INSPIRE, and S. K. thanks IIT Madras for fellowships. We thank Dr P. K. S. Antharjanam, V. Ramkumar, and Dr B. Varghese, DST and SC-XRD LAB, SAIF, IIT Madras for single crystal X-ray diffraction data collection, structure refinement and discussion. The computational facility at IIT Madras is gratefully acknowledged.

Notes and references

- 1 K. Wade, *J. Chem. Soc. D*, 1971, 792–793.
- 2 (a) J. Zhang and Z. Xie, *Chem.-Asian J.*, 2010, **5**, 1742–1757; (b) J. D. Kennedy, *Prog. Inorg. Chem.*, 1986, **34**, 211–434; (c) T. P. Fehlner, J.-F. Halet and J.-Y. Saillard, *Molecular Clusters. A Bridge to Solid State Chemistry*, Cambridge University Press, Cambridge, United Kingdom, 2007; (d) R. N. Grimes, *Carboranes*, Elsevier, Oxford, 3rd edn, 2016; (e) S. Kar and S. Ghosh, Borane Polyhedra beyond Icosahedron, in *50th Anniversary of Electron Counting Paradigms for Polyhedral Molecules. Structure and Bonding*, ed. D. M. P. Mingos, Springer, Berlin, 2021, vol. 187, pp. 109–138; (f) J. D. Kennedy, *Coord. Chem. Rev.*, 2016, **323**, 71–86.
- 3 (a) S. Kar, A. N. Pradhan and S. Ghosh, in *Polyhedral Metallaboranes and Metallacarboranes, Comprehensive Organometallic Chemistry IV*, ed. G. Parkin, K. Meyer and D. O'hare, Elsevier, Amsterdam, 2022, vol. 9, pp. 263–369; (b) G.-X. Jin, *Coord. Chem. Rev.*, 2004, **248**, 587–602; (c) N. S. Hosmane, *Boron Science: New Technologies and Applications*, CRC, Boca Raton, FL, 2011; (d) D. F. Shriver, H. D. Kaesz and R. D. Adams, *The Chemistry of Metal Cluster Complexes*, VCH, New York, 1990; (e) D. Patel, B. S. Sooraj, K. Kirakci, J. Machacek, M. Kučeráková, J. Bould, M. Dusek, M. Frey, C. Neumann, S. Ghosh, A. Turchanin, T. Pradeep and T. Base, *J. Am. Chem. Soc.*, 2023, **145**, 17975–17986; (f) K. O. Kirlikovali, J. A. Axtell, A. Gonzalez, A. C. Phung, S. I. Khan and A. M. Spokoyny, *Chem. Sci.*, 2016, **7**, 5132–5138.
- 4 (a) R. E. Williams, *Inorg. Chem.*, 1971, **10**, 210–214; (b) K. Wade, *Inorg. Nucl. Chem. Lett.*, 1972, **8**, 559–562; (c) K. Wade, *Adv. Inorg. Chem. Radiochem.*, 1976, **18**, 1–66; (d) D. M. P. Mingos, *Acc. Chem. Res.*, 1984, **17**, 311–319; (e) E. D. Jemmis, M. M. Balakrishnarajan and P. D. Pancharatna, *J. Am. Chem. Soc.*, 2001, **123**, 4313–4323.
- 5 R. Hoffmann, *Angew. Chem., Int. Ed. Engl.*, 1982, **21**, 711–724.
- 6 (a) S. Kar, A. N. Pradhan and S. Ghosh, *Coord. Chem. Rev.*, 2021, **436**, 213796; (b) S. Ghosh, B. C. Noll and T. P. Fehlner, *Dalton Trans.*, 2008, 371–378; (c) R. Borthakur, S. Kar, S. K. Barik, S. Bhattacharya, G. Kundu, B. Varghese and S. Ghosh, *Inorg. Chem.*, 2017, **56**, 1524; (d) X. Lei, M. Shang and T. P. Fehlner, *Chem.-Eur. J.*, 2000, **6**, 2653–2664.
- 7 (a) C. W. Jung, R. T. Baker, C. B. Knobler and M. F. Hawthorne, *J. Am. Chem. Soc.*, 1980, **102**, 5782–5790; (b) C. W. Jung, R. T. Baker and M. F. Hawthorne, *J. Am. Chem. Soc.*, 1981, **103**, 810–816; (c) J. Bould, J. D. Kennedy and M. Thornton-Pett, *J. Chem. Soc., Dalton Trans.*, 1992, 563–576; (d) B. Štíbr, J. D. Kennedy, E. Drdáková and M. Thornton-Pett, *J. Chem. Soc., Dalton Trans.*, 1994, 229–236; (e) R. T. Baker, *Inorg. Chem.*, 1986, **25**, 109–111.
- 8 (a) B. Le Guennic, H. Jiao, S. Kahlal, J.-Y. Saillard, J.-F. Halet, S. Ghosh, M. Shang, A. M. Beatty, A. L. Rheingold and T. P. Fehlner, *J. Am. Chem. Soc.*, 2004, **126**, 3203–3217; (b) S. Ghosh, A. M. Beatty and T. P. Fehlner, *Angew. Chem., Int. Ed.*, 2003, **42**, 4678–4680; (c) S. Kar, S. Bairagi, A. Haridas, G. Joshi, E. D. Jemmis and S. Ghosh, *Angew. Chem., Int. Ed.*, 2022, **61**, e202208293; (d) S. Kar, S. Bairagi, K. Saha, B. Raghavendra and S. Ghosh, *Dalton Trans.*, 2019, **48**, 4203–4210; (e) S. Kar, S. Bairagi, J.-F. Halet and S. Ghosh, *Chem. Commun.*, 2023, **59**, 11676–11679.
- 9 (a) W. N. Lipscomb, A. R. Pitochelli and M. F. Hawthorne, *J. Am. Chem. Soc.*, 1959, **81**, 5833–5834; (b) W. L. Lipscomb, in *Boron Hydrides*, Benjamin, New York, 1963; (c) E. L. Muetterties, in *Boron Hydride Chemistry*, Academic Press, New York, 1975; (d) S. Kar, S. Bairagi, G. Joshi, E. D. Jemmis and S. Ghosh, *Chem.-Eur. J.*, 2021, **27**, 15634–15637.
- 10 E. D. Jemmis, *J. Am. Chem. Soc.*, 1982, **104**, 7017–7020.
- 11 (a) R. B. King, *Inorg. Chem.*, 1999, **38**, 5151–5153; (b) R. L. Johnston and D. M. P. Mingos, *Inorg. Chem.*, 1986, **25**, 3321–3323.
- 12 K. P. Callahan, W. J. Evans, F. Y. Lo, C. E. Strouse and M. F. Hawthorne, *J. Am. Chem. Soc.*, 1975, **97**, 296–302.
- 13 (a) W. N. Lipscomb, *Science*, 1966, **153**, 373–378; (b) R. B. King, *Inorg. Chim. Acta*, 1981, **49**, 237–240.
- 14 J. E. Crook, M. Elrington, N. N. Greenwood, J. D. Kennedy, M. Thornton-Pett and J. D. Woollins, *J. Chem. Soc., Chem. Commun.*, 1985, 2407–2415.
- 15 J. Bould, J. E. Crook, N. N. Greenwood, J. D. Kennedy and W. S. McDonald, *J. Chem. Soc., Dalton Trans.*, 1982, 346–348.
- 16 R. Borthakur, B. Mondal, P. Nandi and S. Ghosh, *Chem. Commun.*, 2016, **52**, 3199–3202.
- 17 H. Kameo and H. Suzuki, *Organometallics*, 2008, **27**, 4248–4253.
- 18 (a) J. Bould, N. N. Greenwood and J. D. Kennedy, *J. Organomet. Chem.*, 1983, **249**, 11–21; (b) J. Bould, M. G. S. Londesborough, V. Passarelli, W. Clegg,



- P. G. Waddell, J. Cvačka and R. Macías, *Dalton Trans.*, 2021, **50**, 16751–16764; (c) A. N. Simonov, J. F. Boas, M. A. Skidmore, C. M. Forsyth, E. Mashkina, M. Bown and A. M. Bond, *Inorg. Chem.*, 2015, **54**, 4292–4302.
- 19 D. K. Roy, R. Borthakur, R. Prakash, S. Bhattacharya, R. Jagan and S. Ghosh, *Inorg. Chem.*, 2016, **55**, 4764–4770.
- 20 (a) R. B. King, *Inorg. Chem.*, 2006, **45**, 8211–8216; (b) R. B. King and S. Ghosh, *Theor. Chem. Acc.*, 2012, **131**, 1087; (c) A. Lupana and R. B. King, *New J. Chem.*, 2013, **37**, 2528–2536.
- 21 A. S. Weller, M. Shang and T. P. Fehlner, *Chem. Commun.*, 1998, 1787–1788.

